

# Graded functional diffusion map–defined characteristics of apparent diffusion coefficients predict overall survival in recurrent glioblastoma treated with bevacizumab

Benjamin M. Ellingson, Timothy F. Cloughesy, Albert Lai, Paul S. Mischel, Phioanh L. Nghiemphu, Shadi Lalezari, Kathleen M. Schmainda, and Whitney B. Pope

*Department of Radiological Sciences, David Geffen School of Medicine, University of California Los Angeles, Los Angeles, CA (B.M.E., W.B.P.); Department of Neurology, David Geffen School of Medicine, University of California Los Angeles, Los Angeles, CA (T.F.C., A.L., P.L.N., S.L.); Department of Pathology and Laboratory Medicine, David Geffen School of Medicine, University of California Los Angeles, Los Angeles, CA (P.S.M.); Departments of Radiology and Biophysics, Medical College of Wisconsin, Milwaukee, WI (K.M.S.)*

Diffusion imaging has shown promise as a predictive and prognostic biomarker in glioma. We assessed the ability of graded functional diffusion maps (fDMs) and apparent diffusion coefficient (ADC) characteristics to predict overall survival (OS) in recurrent glioblastoma multiforme (GBM) patients treated with bevacizumab. Seventy-seven patients with recurrent GBMs were retrospectively examined. MRI scans were obtained before and approximately 6 weeks after treatment with bevacizumab. Graded fDMs were created by registering datasets to each patient's pretreatment scan and then performing voxel-wise subtraction between post- and pretreatment ADC maps. Voxels were categorized according to the degree of change in ADC within pretreatment fluid-attenuated inversion recovery (FLAIR) and contrast-enhancing regions of interest (ROIs). We found that the volume of tissue showing decreased ADC within both FLAIR and contrast-enhancing regions stratified OS (log-rank,  $P < .05$ ). fDMs applied to contrast-enhancing ROIs more accurately predicted OS compared with fDMs applied to FLAIR ROIs. Graded fDMs (showing voxels with decreased ADC

between 0.25 and 0.4  $\mu\text{m}^2/\text{ms}$ ) were more predictive of OS than traditional (single threshold) fDMs, and the predictive ability of graded fDMs could be enhanced even further by adding the ADC characteristics from the fDM-classified voxels to the analysis (log-rank,  $P < .001$ ). These results demonstrate that spatially resolved diffusion-based tumor metrics are a powerful imaging biomarker of survival in patients with recurrent GBM treated with bevacizumab.

**Keywords:** diffusion MRI, biomarker, fDM, functional diffusion map, GBM, glioblastoma.

**G**lioblastoma multiforme (GBM) is the most common malignant primary brain tumor, characterized by a very poor patient prognosis. Median survival in patients diagnosed with GBM is approximately 12–14 months with radiation and chemotherapy.<sup>1,2</sup> The high level of tumor vascularity, due partially to secretion of vascular endothelial growth factor (VEGF),<sup>3–5</sup> has generated interest in anti-VEGF therapies aimed at reducing tumor angiogenesis. Initial clinical trials have shown an increased progression-free survival in patients treated with the humanized monoclonal VEGF-blocking antibody bevacizumab<sup>6–8</sup> compared with historical controls.<sup>1</sup> These results were based on modified Macdonald criteria,<sup>9</sup> which are limited in the evaluation of anti-angiogenic treatments due to the effect of these drugs on vascular permeability and the volume of contrast agent extravasation.<sup>10,11</sup>

Received December 17, 2010; accepted April 29, 2011.

**Corresponding Author:** Benjamin M. Ellingson, Ph.D., Assistant Professor, Department of Radiological Sciences, David Geffen School of Medicine, University of California Los Angeles, 924 Westwood Blvd., Suite 650, Los Angeles, CA 90024 (bellingson@mednet.ucla.edu).

Therefore, we have investigated the application of a diffusion-sensitive MRI biomarker, the functional diffusion map (fDM), as an early predictor of bevacizumab response in recurrent GBM.

The fDM technique was developed in order to examine localized differences in diffusion (change in apparent diffusion coefficient [ADC] [ $\Delta$ ADC]) measured in the same patient over time, in order to prevent averaging of all tumor ADC values that might obscure potentially relevant changes occurring within subportions of the tumor.<sup>12–16</sup> This technique has demonstrated utility in predicting the effect of cytotoxic chemotherapy and radiotherapy within the contrast-enhancing tumor bed<sup>12–15</sup> as well as within regions of abnormal fluid-attenuated inversion recovery (FLAIR) signal.<sup>16–18</sup> Additionally, this method has shown promise in the evaluation of anti-angiogenic therapies.<sup>19,20</sup>

In the current study, we use a modified fDM technique proposed by Ellingson et al.<sup>17</sup> using graded thresholds that may reflect differing degrees of cell density change. These graded fDMs computed from pre- and posttreatment ADC maps were evaluated for their ability to serve as predictors of survival in patients with recurrent GBM treated with bevacizumab.

In contrast to the “traditional” fDM approach, the graded fDM technique allows quantification and tracking of the volume of tissue showing changes *between* different  $\Delta$ ADC thresholds. Bevacizumab significantly reduces vasogenic edema; therefore, we hypothesized that regions of the brain containing either solid or infiltrating tumor plus edema are likely to exhibit less of a decrease in ADC following bevacizumab treatment compared with regions containing a larger proportion of edema (Fig. 1). By using graded fDMs, these more subtle differences in ADC can be visualized and quantified and may relate to pretreatment tumor burden. Therefore, we hypothesized that pretreatment ADC distributions within the graded fDM-categorized regions could be a useful biomarker to stratify survival in patients with recurrent GBM treated with bevacizumab.

## Methods

### Patients

All patients participating in this study signed institutional review board–approved informed consent to have their data collected and stored in our institution’s neuro-oncology database. Data acquisition was performed in compliance with all applicable regulations of the Health Insurance Portability and Accountability Act (HIPAA). The study spanned November 15, 2005 to August 31, 2010. Patients were retrospectively selected from our institution’s neuro-oncology database. A total of  $n = 252$  patients who met the following criteria were initially selected: (1) had pathologically confirmed GBM with recurrence based on MRI, abnormal uptake of 3,4-dihydroxy-6-<sup>[18F]</sup>-fluoro-L-phenylalanine (<sup>18F</sup>-FDOPA) PET, clinical data and/or histology, (2)

were regularly treated every 2 weeks per cycle with bevacizumab (Avastin, Genentech; 5 or 10 mg/kg body weight) alone or in combination with chemotherapy (carboplatin, irinotecan, etoposide, lomustine), (3) had baseline (pre-bevacizumab treatment) and minimum of 1 follow-up MRI scan, and (4) had treatment with bevacizumab at least 3 months postradiotherapy to reduce the probability of pseudoprogression and treatment-induced necrosis. Of these patients,  $n = 77$  had good-quality diffusion-weighted images before and after initiation of bevacizumab treatment. A total of 40 of 77 patients had histologically confirmed GBM. A total of 47 of 77 patients (61%) were administered bevacizumab more than 12 months after completion of radiotherapy. Of the patients who were administered bevacizumab within 12 months of radiotherapy, recurrence was confirmed using either direct pathology, <sup>18F</sup>-FDOPA PET, or unequivocal evidence on MRI as indicated by a board-certified neuroradiologist (W.B.P.). Unequivocal evidence on MRI was determined by more than 2 sequential months of increasing contrast enhancement on postcontrast T1-weighted MRI, along with evidence of increasing mass effect. Baseline scans were obtained approximately 1.5 weeks pretreatment (mean = 11 d  $\pm$  1.6 d, standard error of the mean [SEM]). Follow-up scans were obtained at approximately 6 weeks posttreatment (mean = 42 d  $\pm$  3.5 d SEM). At the time of last assessment (August 2010), 63 of the 77 patients were deceased. For bevacizumab-treated patients, 33 patients were on steroids at the time of initial imaging (dose range 0.25–24 mg dexamethasone) and 44 patients were not on steroids. Of the 33 patients on steroids, 18 patients had no change in dose between the MRI scans examined; 10 patients had a decrease in steroid dose; and 5 patients had an increase in steroid dose. A total of 52 patients were treated at first recurrence, 20 at second recurrence, and 5 at third or more recurrence. All patients were treated with radiation therapy (typically 6000 cGy) and maximal tumor resection at time of initial tumor presentation.

### MRI

Data were collected on a 1.5T MR system (General Electric Medical Systems) using pulse sequences supplied by the scanner manufacturer. Standard anatomical MRI sequences included axial T1-weighted (echo time/repetition time (TE/TR) = 15 ms/400 ms, slice thickness = 5 mm with 1-mm interslice distance, number of excitations (NEX) = 2, matrix size = 256  $\times$  256, and field of view (FOV) = 24 cm), T2-weighted fast spin-echo (TE/TR = 126–130 ms/4000 ms, slice thickness = 5 mm with 1-mm interslice distance, NEX = 2, matrix size = 256  $\times$  256, and FOV = 24 cm), and FLAIR images (inversion time = 2200 ms, TE/TR = 120 ms/4000 ms, slice thickness = 5 mm with 1-mm interslice distance, NEX = 2, matrix size = 256  $\times$  256, and FOV = 24 cm). Diffusion-weighted images were collected with TE/TR = 102.2 ms/8000 ms, NEX = 1, slice thickness = 5 mm with 1-mm interslice distance, matrix size = 128  $\times$  128

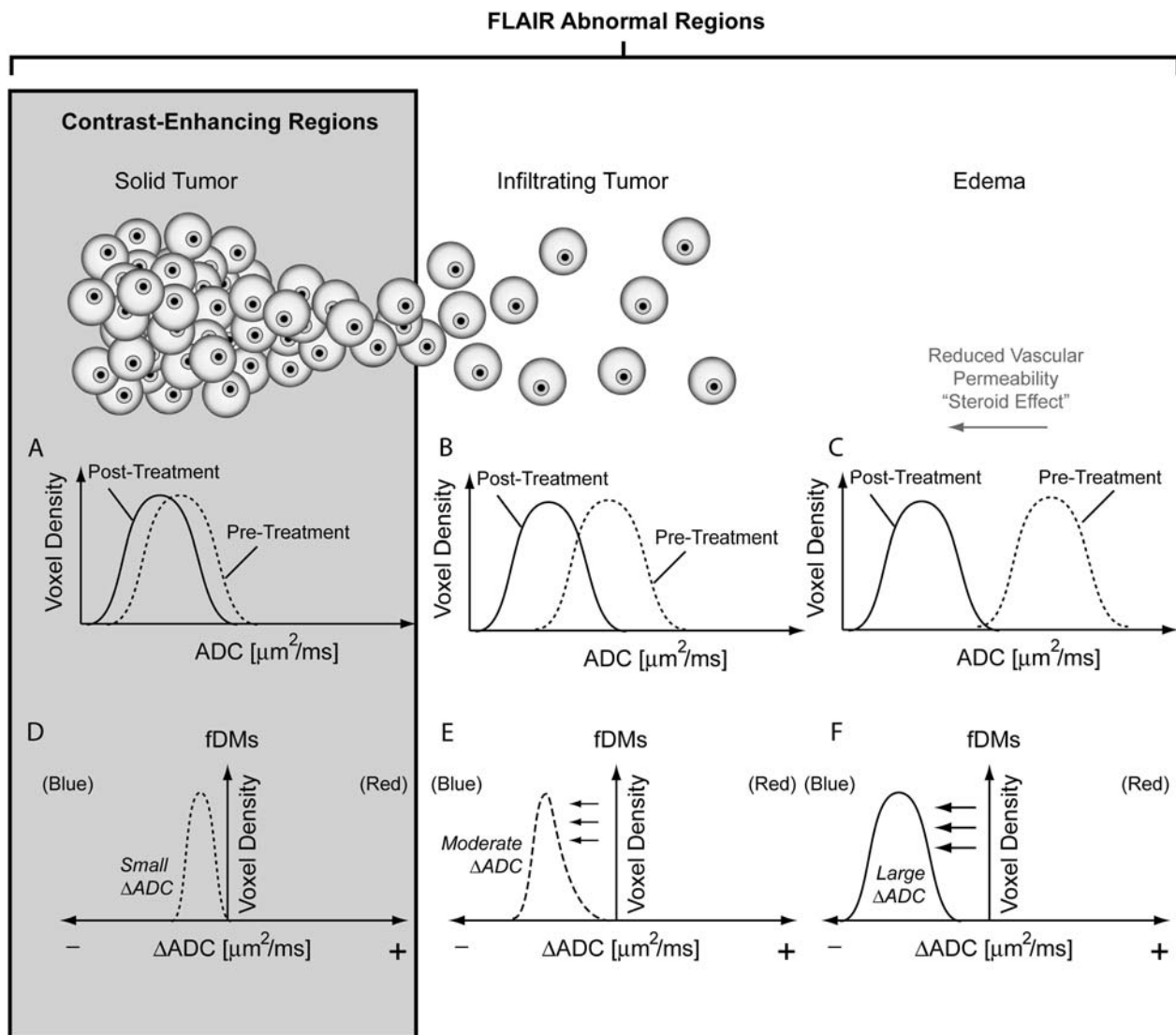


Fig. 1. Expected changes in apparent diffusion coefficient (ADC) after treatment with bevacizumab. At the first time point posttreatment, regions containing solid tumor are expected to have a small  $\Delta\text{ADC}$  (A), whereas regions containing infiltrating tumor (B) or edema (C) are expected to have a relatively large  $\Delta\text{ADC}$ . This  $\Delta\text{ADC}$  is quantified on a voxel-wise basis by setting small (D), moderate (E), and large (F)  $\Delta\text{ADC}$  thresholds on fDMs. FLAIR regions are expected to contain a mixture of solid tumor, infiltrating tumor, and edema, whereas regions of contrast enhancement are expected to contain primarily solid, viable tumor.

(reconstructed images were zero-padded and interpolated to  $256 \times 256$ ), and FOV = 24 cm using a twice-refocused spin-echo echo planar preparation.<sup>21</sup> ADC images were calculated from acquired diffusion-weighted images with  $b = 1000 \text{ s/mm}^2$  and  $b = 0 \text{ s/mm}^2$  images. Additionally, gadopentetate dimeglumine-enhanced (Magnevist; Berlex; 0.1 mmol/kg) axial and coronal T1-weighted images (coronal: TE/TR = 15 ms/400 ms, slice thickness 3 mm with 1-mm interslice distance, NEX = 2, matrix size  $256 \times 256$ , FOV = 24 cm) were acquired immediately after contrast injection.

#### Image Registration

All images for each patient were registered to baseline anatomical T1-weighted images using a mutual

information algorithm and a 12-degree-of-freedom transformation using the FMRIB Software Library Functional Magnetic Resonance Imaging of the Brain Analysis Group, Oxford University (<http://www.fmrib.ox.ac.uk/fsl/>). Fine registration (1–2 degrees and 1–2 voxels) was then performed using a Fourier transform-based, 6-degree-of-freedom, rigid body registration algorithm<sup>22</sup> followed by visual inspection to ensure adequate alignment. Similar registration techniques were used in previous fDM studies.<sup>14–17</sup>

#### Graded fDM Calculation

After proper registration was visually verified, voxel-wise subtraction was performed between (1) ADC maps acquired posttreatment and (2) baseline, pretreatment

ADC maps. Individual voxels were stratified into 6 categories based on the change in ADC relative to the baseline ADC map. Dark red voxels represented areas where ADC increased beyond a  $\Delta\text{ADC}$  threshold of  $0.75 \mu\text{m}^2/\text{ms}$ , orange voxels represented areas where ADC increased beyond a  $\Delta\text{ADC}$  threshold of  $0.4 \mu\text{m}^2/\text{ms}$ , and light orange voxels represented areas where ADC increased beyond a  $\Delta\text{ADC}$  threshold of  $0.25 \mu\text{m}^2/\text{ms}$ . Together, these 3 thresholds are generically referred to as *levels of increasing ADC*. Dark blue voxels represented areas where ADC decreased beyond a  $\Delta\text{ADC}$  threshold of  $0.75 \mu\text{m}^2/\text{ms}$ , blue voxels represented areas where ADC decreased beyond a  $\Delta\text{ADC}$  threshold of  $0.4 \mu\text{m}^2/\text{ms}$ , and light blue voxels represented areas where ADC decreased beyond a  $\Delta\text{ADC}$  threshold of  $0.25 \mu\text{m}^2/\text{ms}$ . Together, these 3 thresholds are generically referred to as *levels of decreasing ADC*.

These  $\Delta\text{ADC}$  thresholds ( $\pm 0.75 \mu\text{m}^2/\text{ms}$ ,  $\pm 0.40 \mu\text{m}^2/\text{ms}$ , and  $\pm 0.25 \mu\text{m}^2/\text{ms}$ ) represent the 95% confidence interval (CI) for different tissue mixtures (gray matter, white matter, and cerebrospinal fluid in the subarachnoid space within sulci) previously evaluated within normal-appearing brain tissue in 69 patients with various tumor grades and time intervals ranging from 1 week to 1 year postbaseline.<sup>17</sup> Additionally, these thresholds have been calibrated with respect to change in cell density in treatment-naïve gliomas (approximately  $\pm 7426$  nuclei/ $\text{mm}^2$ ,  $\pm 3960$  nuclei/ $\text{mm}^2$ , and  $\pm 2475$  nuclei/ $\text{mm}^2$ ) reported in a previous publication.<sup>17</sup>

#### Quantification of fDM Tissue Subtypes

Using the traditional fDM approach, the physical volume (in cc) of fDM-classified tissue subtypes was calculated for posttreatment fDMs using a single  $\Delta\text{ADC}$  threshold of  $0.40 \mu\text{m}^2/\text{ms}$ , which has been shown to correspond to the 95% CI for  $\Delta\text{ADC}$  for a mixture of gray and white matter in 69 patients evaluated from 1 week to 1 year postbaseline, is recommended for the best balance between sensitivity and specificity to progressing disease, and corresponds to an estimated change in cell density beyond  $\pm 3960$  nuclei/ $\text{mm}^2$ .<sup>17</sup> In addition to calculating the physical volume of tissue with ADC *beyond* this threshold, as per the traditional fDM technique, we also determined the physical volume of tissue having  $\Delta\text{ADC}$  *between*  $0.25 \mu\text{m}^2/\text{ms}$  and  $0.40 \mu\text{m}^2/\text{ms}$ , corresponding to light blue regions on graded fDMs, which we hypothesize may more accurately reflect tumor burden within pretreatment FLAIR regions of interest (ROIs). Based on the noise distributions within a mixture of normal-appearing gray and white matter reported in an earlier fDM publication,<sup>17</sup> we estimated a 7.5% probability of obtaining a decrease in ADC between  $0.25 \mu\text{m}^2/\text{ms}$  and  $0.40 \mu\text{m}^2/\text{ms}$  simply by chance.

#### Region of Interest Determination

In the current study, we chose to apply the traditional and graded fDM techniques to regions of signal abnormality on pretreatment FLAIR images as well as regions of

contrast enhancement on postcontrast T1-weighted images in order to provide a comprehensive comparison. FLAIR ROIs<sup>16–20</sup> and contrast-enhancing ROIs<sup>12–15</sup> have both previously been used in interpreting fDM results. We used a semi-automated process consisting of (1) manually defining the relative region of tumor occurrence, (2) thresholding either the FLAIR or postcontrast images using an empirical threshold combined with a region-growing algorithm, and (3) manually editing the resulting masks to exclude any obvious errors.

#### Hypothesis Testing

We hypothesized that fDMs generated posttreatment would result in a substantial volume of decreased ADC due to the substantial decrease in edema reported during anti-angiogenic treatment<sup>11,23</sup> and potentially due to tumor growth (increase in number and density of cells) between the pre- and posttreatment scan dates, resulting in a larger volume of decreased ADC in patients who were at risk for treatment failure compared with those who had more favorable response. To test this hypothesis, we performed a log-rank statistical analysis on Kaplan–Meier data to determine whether stratifying the patients according to the physical volume of fDM-classified decreasing ADC, using a single  $\Delta\text{ADC}$  threshold of  $0.40 \mu\text{m}^2/\text{ms}$ , was a significant predictor of overall survival (OS) from initiation of bevacizumab treatment. Then, using the graded fDM technique, we quantified the volume of tissue with a change in ADC *between* different thresholds and tested whether the physical volume of tissue exhibiting a decrease in ADC *between*  $0.25$  and  $0.40 \mu\text{m}^2/\text{ms}$ , which we hypothesize may more accurately reflect tumor burden (see Fig. 1), was a significant predictor of OS with respect to the initiation of bevacizumab treatment.

In order to verify that voxels classified using the graded fDM technique represented a significantly different subpopulation of voxels compared with traditional fDM classifications and the entire ROI in general, we utilized a chi-squared goodness-of-fit test to compare ADC distributions between these different categorizations. Specifically, for each patient, we performed a chi-squared test comparing the observed ADC probability density function from the graded fDM-classified regions with the expected ADC probability density function within the entire ROI (FLAIR or contrast-enhancing), as well as comparing the observed probability density function from the graded fDM-classified regions with the expected ADC probability density function extracted by traditional fDM classification using in-house MATLAB algorithms (Mathworks). We then tested whether graded fDMs combined with ADC characteristics from fDM-classified voxels could better predict survival compared with fDMs alone.

## Results

For all patients who expired in the current study (63 of 77 patients), the mean OS was 317 days  $\pm$  20 days

SEM (median OS = 285 d) from the time of the first bevacizumab treatment. At the first follow-up time point from bevacizumab treatment, approximately 85% (66/77) of patients exhibited a reduction (>5%) in the extent of FLAIR signal abnormality and approximately 85% (66/77) exhibited a decrease (>5%) in contrast-enhancing tumor volume. Approximately 90% (69/77) of patients examined had either a reduction in contrast enhancement or a reduction in FLAIR signal abnormality, whereas 10% (8/77) of the patients had no significant radiographic response.

### Traditional fDMs

The fDM technique typically applies a single  $\Delta\text{ADC}$  threshold to classify voxels into increasing or decreasing ADC. In order to determine whether the physical volume of decreasing ADC classified using the traditional fDM technique with  $\Delta\text{ADC} = 0.4 \mu\text{m}^2/\text{ms}$  was a significant predictor of OS, we performed log-rank analysis on Kaplan–Meier curves for both FLAIR and contrast-enhancing ROIs (Figs. 2 and 3). In general, patients exhibiting a higher volume of tissue with decreased ADC appeared to have a shorter OS. When applying a threshold of  $0.40 \mu\text{m}^2/\text{ms}$ , which is recommended for traditional fDM analysis for the best

balance of sensitivity and specificity to progressing disease,<sup>17</sup> we observed a significant survival advantage in patients with a volume of tissue having decreased ADC above the median volume of 13 cc (Fig. 3A; log-rank,  $P = .0030$ ; hazard ratio (HR) = 1.976, 95% CI for HR = 1.318–3.866). For the traditional fDM technique applied to FLAIR ROIs, the sensitivity and specificity for correctly classifying 6-month OS were 78.6% and 57.1%, respectively, and the sensitivity and specificity for classifying 12-month OS were 56% and 63% (Table 1). Traditional fDM-classified voxels within regions of contrast enhancement also demonstrated a significant survival advantage for patients exhibiting a volume of tissue with decreasing ADC greater than the group median of 2 cc (Fig. 3B; log-rank,  $P = .0013$ ; HR = 2.079, 95% CI/HR = 1.417–4.248). The sensitivity and specificity to accurately classify patients based on 6-month OS were 71% and 56%, respectively, whereas the sensitivity and specificity of traditional fDM classification in regions of contrast enhancement to 12-month OS were 60% and 70%, respectively (Table 1). Other methods of applying traditional fDM analysis, including the volume of tissue with increasing ADC, volume of tissue with any  $\Delta\text{ADC}$  (increasing or decreasing ADC), and fractional volumes changing ADC within FLAIR

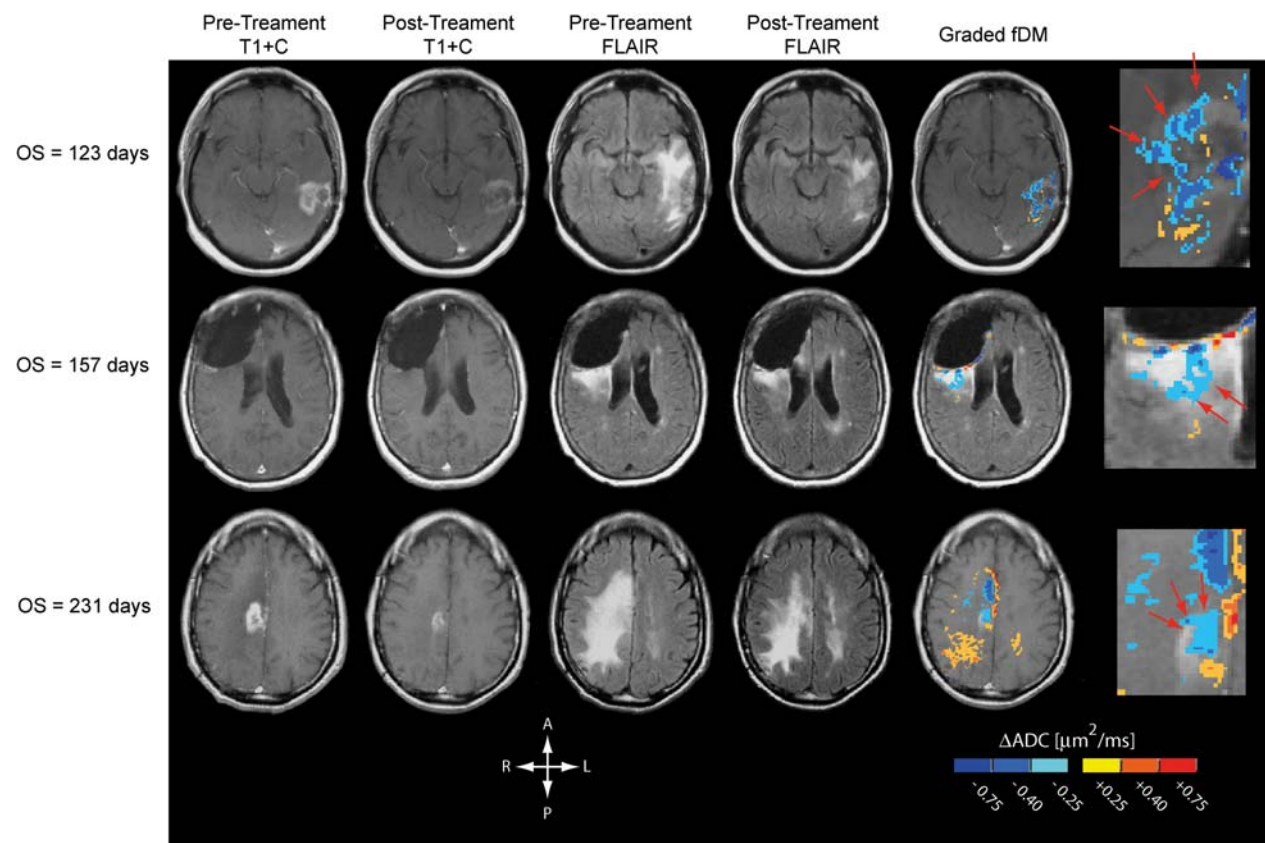


Fig. 2. Postcontrast T1-weighted images, FLAIR images, and graded fDMs in recurrent GBM patients treated with bevacizumab. From left column: pretreatment, postcontrast T1-weighted images; posttreatment, postcontrast T1-weighted images; pretreatment FLAIR images; posttreatment FLAIR images; graded fDMs; zoomed-in region of graded fDMs showing areas of subtle ADC decrease localized to regions of contrast enhancement that may represent residual tumor burden (arrows). Rows are ordered with respect to increasing OS.

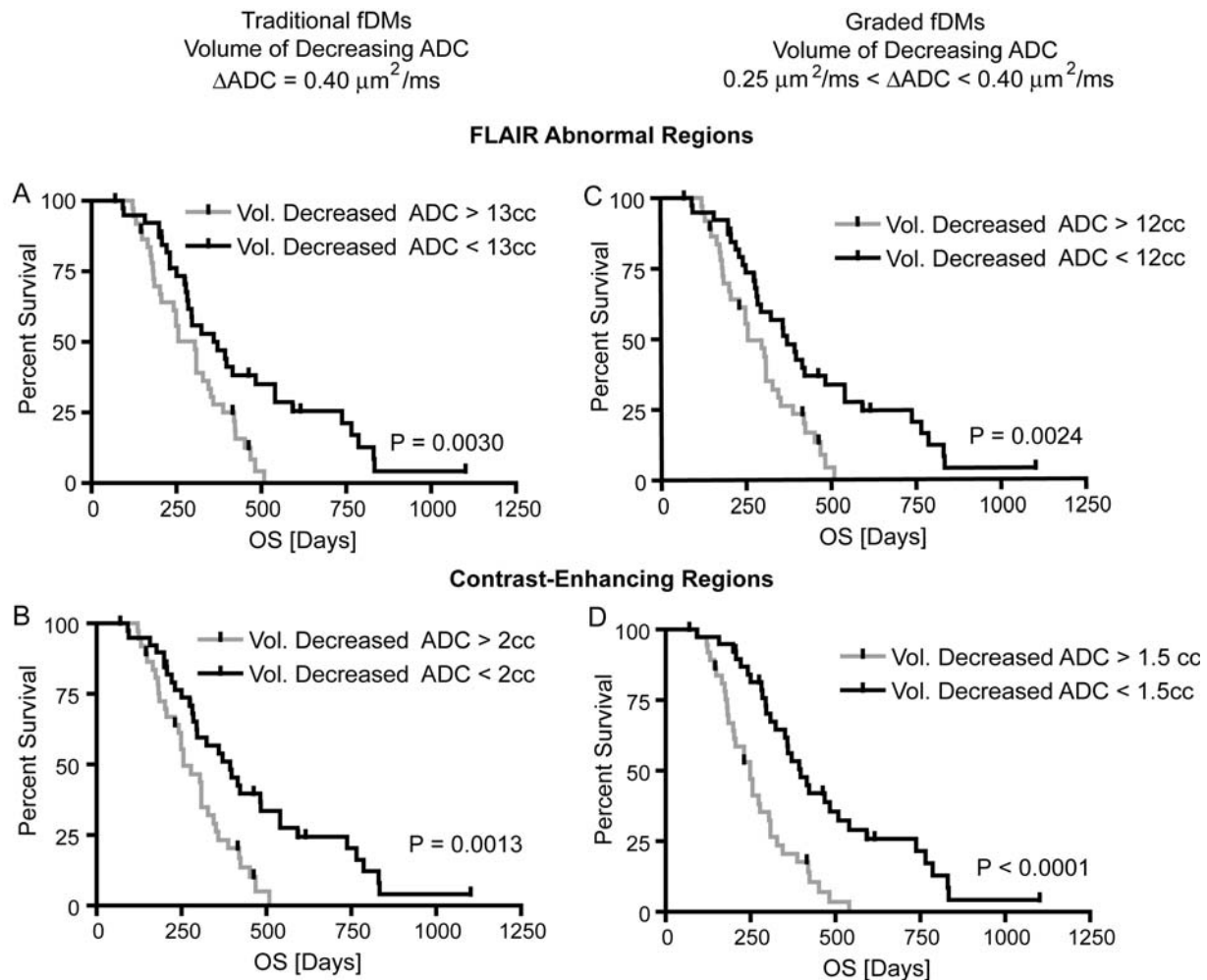


Fig. 3. Kaplan–Meier curves showing effect of fDM-classified decreasing ADC volumes on OS. In general, both traditional and graded fDMs applied to either FLAIR or contrast-enhancing regions were able to significantly stratify patients into short- and long-term OS. (A) Traditional fDM technique applied to FLAIR ROIs shows significant survival advantage in patients having a volume of decreasing ADC less than the group median of 13 cc (log-rank,  $P = .003$ ; median OS: 304 vs. 371 d). (B) Similarly, the traditional fDM technique applied to contrast-enhancing ROIs shows significant survival advantage in patients having a volume of decreasing ADC less than the group median of 2 cc (log-rank,  $P = .0013$ ; median OS: 256 vs. 393 d). (C) Using graded fDM classification, we also observed a survival advantage in patients showing a volume of decreasing ADC between  $0.25 \mu\text{m}^2/\text{ms}$  and  $0.4 \mu\text{m}^2/\text{ms}$  larger than the group median of 12 cc (log-rank,  $P = .0024$ ; median OS: 256 vs. 371 d). (D) Within contrast-enhancing ROIs, patients showing a volume of decreasing ADC between  $0.25 \mu\text{m}^2/\text{ms}$  and  $0.4 \mu\text{m}^2/\text{ms}$  larger than the group median of 1.5 cc also had a survival advantage (log-rank,  $P < .0001$ ; median OS: 249 vs. 397 d).

or contrast-enhancing ROIs, were not found to be predictive (log-rank,  $P > .05$ ; results not shown).

#### Graded fDMs

The use of graded fDM classification allowed for slightly improved stratification of patients with respect to survival compared with the traditional fDM approach (Fig. 3C and D). Consistent with our original hypothesis, patients with a volume of tissue having a decrease in ADC within the range of  $0.25$  and  $0.4 \mu\text{m}^2/\text{ms}$  larger than the group median of 12 cc within FLAIR ROIs were more likely to expire sooner than patients with

lower volumes (Fig. 3C; log-rank,  $P = .0024$ ; HR = 2.012, 95% CI/HR = 1.35–4.0). The sensitivity and specificity of graded fDMs applied to FLAIR ROIs to predict 6-month OS were 79% and 57%, respectively, whereas the sensitivity and specificity of graded fDMs applied to FLAIR ROIs to predict 12-month OS were 58% and 67%, respectively (Table 1). Patients having a volume of tissue exhibiting a decrease in ADC within the range of  $0.25$  and  $0.4 \mu\text{m}^2/\text{ms}$  larger than the group median of 1.5 cc within contrast-enhancing ROIs had a significantly shorter survival compared with patients having a lower volume (Fig. 3D; log-rank,  $P < .0001$ ; HR = 2.679, 95% CI/HR = 1.987–6.136). The sensitivity and specificity for

**Table 1.** Summary of survival analyses for different fDM techniques and regions of interest

fDM Technique	ROI	Hazard Ratio (HR)	95% CI for HR	Sensitivity to 6-month OS (%)	Specificity to 6-month OS (%)	Sensitivity to 12-month OS (%)	Specificity to 12-month OS (%)
Traditional fDM	Contrast enhanced	2.079	1.417–4.248	71.0	56.0	60.0	70.0
Graded fDM	Contrast enhanced	2.679	1.987–6.136	86.0	59.0	62.0	74.0
Traditional fDM	FLAIR	1.976	1.318–3.866	78.6	57.1	56.0	63.0
Graded fDM	FLAIR	2.012	1.350–4.000	79.0	57.0	58.0	67.0
Mode of ADC in graded fDM	Contrast enhanced	3.262	2.880–9.110	78.0	68.2	81.5	89.5
Mode of ADC in graded fDM	FLAIR	1.3918	0.861–2.312	49.2	46.2	63.9	58.0

graded fDMs applied to contrast-enhancing ROIs to predict 6-month OS were 86% and 59%, respectively, and the sensitivity and specificity to predict 12-month OS were 62% and 74%, respectively (Table 1). In general, both traditional and graded fDMs applied to either region were predictive of OS; however, regions of contrast enhancement had higher sensitivity and specificity compared with FLAIR regions. Additionally, the graded fDM technique had higher sensitivity and specificity for 6-month and 12-month OS compared with traditional fDMs in all ROIs evaluated.

#### *Graded fDMs Reflect Significantly Different Voxel Populations*

In order to test whether graded fDM classification extracted a significantly different voxel subpopulation compared with traditional fDMs and the entire ROI, we compared the ADC probability density functions between these ROIs in all 77 patients. Results suggest that graded fDM-classified ADC distributions within regions of contrast enhancement were significantly different from ADC distributions within the entire region of contrast enhancement for nearly 60% (46/77) of patients and were significantly different from ADC distributions for traditional fDM-classified voxels in 66% (51/77) of patients (chi-squared goodness-of-fit,  $P < .05$ ). Results were visually similar for FLAIR ROIs, and so FLAIR regions were not tested statistically. Figure 4 illustrates 4 typical patients with different OS. Visually, the ADC histograms appear different for each of the classification schemes (traditional fDMs, graded fDMs, and the entire contrast-enhancing ROI). Also, the ADC distributions extracted from graded fDM regions appear to be “filtered” with respect to the entire ROI, focusing the ADC distribution into a narrow, quite low ADC peak. Results suggest that for the majority of patients, at least in regions of contrast enhancement, graded fDM classification of voxels having a decrease in ADC within the range of 0.25 and 0.4  $\mu\text{m}^2/\text{ms}$  may represent a unique, statistically different voxel subpopulation.

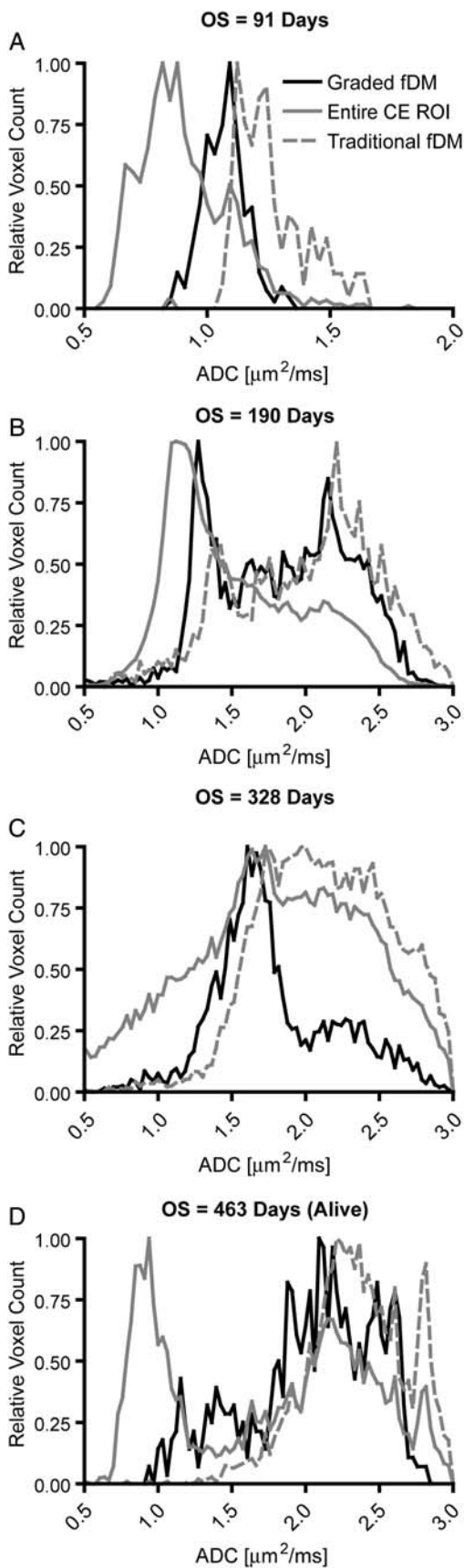
#### *Combining Graded fDMs with ADC Characteristics*

Based on previous work showing the ability of pretreatment ADC distributions to predict progression-free

survival,<sup>24</sup> we hypothesized that the predictive power of the graded fDM technique might be improved through the use of ADC distribution characteristics within these voxel subpopulations. Based on the ADC distributions within the graded fDM classification (as demonstrated in Fig. 4), we chose to measure the distribution “mode” as a measure of central tendency. Results suggest no difference in survival for patients having a mode of ADC within graded fDM-classified voxels lower than the group median value when examining FLAIR ROIs (Fig. 5A; log-rank,  $P = .1715$ ; HR = 1.3918, 95% CI/HR = 0.8613–2.312); however, when examining regions of contrast enhancement, we found a significant survival advantage in patients having a higher mode of ADC within graded fDM-classified voxels compared with patients having a low mode (Fig. 5B; log-rank,  $P < .0001$ , HR = 3.262, 95% CI/HR = 2.88–9.11). For FLAIR ROIs, the sensitivity and specificity to 6-month OS were 49.2% and 46.2%, respectively, whereas the sensitivity and specificity to 12-month OS were 63.9% and 58%, respectively. Within contrast-enhancing ROIs, the sensitivity and specificity to 6-month OS were 78.0% and 68.2%, respectively, whereas the sensitivity and specificity to 12-month OS were 81.5% and 89.5%, respectively (Table 1). Using the 95% CI/HR, the combined biomarker consisting of the mode of the ADC distribution within graded fDM-classified voxels was a significantly better predictor of OS than fDMs or ADC distribution information alone. Additionally, both the sensitivity and specificity of the mode of the ADC distribution within graded fDM-classified voxels to 12-month OS were approximately 20% higher than traditional fDMs or graded fDMs alone. Although these results suggest that graded fDM techniques have descriptively higher HRs than traditional fDM techniques, there is no evidence to formally prove that the differences are statistically significant. However, our results suggest that graded fDM classification combined with ADC distribution information from these classified voxels may be a powerful and unique biomarker for predicting OS in recurrent GBM patients treated with bevacizumab.

## Discussion

The fDM technique has previously been used to predict response to initial cytotoxic therapies and/or



radiotherapies.<sup>15,16,19,20</sup> Since ADC is, in general, believed to be inversely correlated with tumor cell density, a favorable fDM response to cytotoxic therapies and/or radiotherapies is thought to result in a larger volume fraction of tumor moving from a low ADC to a high ADC.<sup>12</sup> Alternatively, an unfavorable fDM response to cytotoxic therapies and/or radiotherapies is thought to result in a larger volume fraction of tumor moving to a lower ADC.<sup>16–18,20</sup> Although this hypothesis is intuitive for cytotoxic therapies and/or radiotherapies that directly destroy tumor cells, this paradigm may not be applicable to the evaluation of the initial response to anti-angiogenic and other cytostatic treatments. Therefore, alternative hypotheses for fDM evaluation of anti-angiogenic treatment are warranted.

#### *Subtle Changes in ADC After Initial Anti-angiogenic Treatment Within Regions of Contrast Enhancement May Reflect Residual Tumor Burden*

Significant reduction in vascular permeability, or a “steroid effect,” is commonly observed following administration of anti-angiogenic therapies.<sup>6,10,11,25</sup> This reduction in vascular permeability results in a decrease in ADC within areas containing edema. In regions containing solid tumor before administration of anti-angiogenic drugs, however,  $\Delta$ ADC due to changes in vascular permeability is likely much smaller.<sup>24</sup> In regions containing a mixture of infiltrative tumor and edema, the response is likely to be a mixture of both the solid-tumor and pure edema responses. Consistent with our initial hypothesis (Fig. 1), we found that both traditional and graded fDMs applied to either FLAIR or contrast enhancement were predictive of OS, where the larger the volume of tissue with decreased ADC, the shorter the OS. Results from the current study also suggest that the volume of decreasing ADC on both graded and traditional fDMs applied to contrast-enhancing regions within the tumor is slightly more predictive of OS than that applied to regions of FLAIR signal abnormality. Additionally, our results demonstrate that the ADC characteristics within

Fig. 4. Representative pre-treatment ADC distributions within different ROIs for OS consisting of (A) 91 days posttreatment, (B) 190 days posttreatment, (C) 328 days posttreatment, and (D) 463 days posttreatment in a long-term survivor. Note the large difference between many of the ADC distributions and a steady shift to higher mode ADC with increasing survival. Solid black lines represent ADC distributions within graded fDM-classified ROIs. Solid gray lines represent ADC distributions within the entire contrast-enhancing ROI. Dashed gray lines represent ADC distributions within traditional fDM-classified ROIs. “Relative voxel count” was defined as the voxel count in a particular bin divided by the maximum voxel count observed in all bins. CE = contrast enhancing.

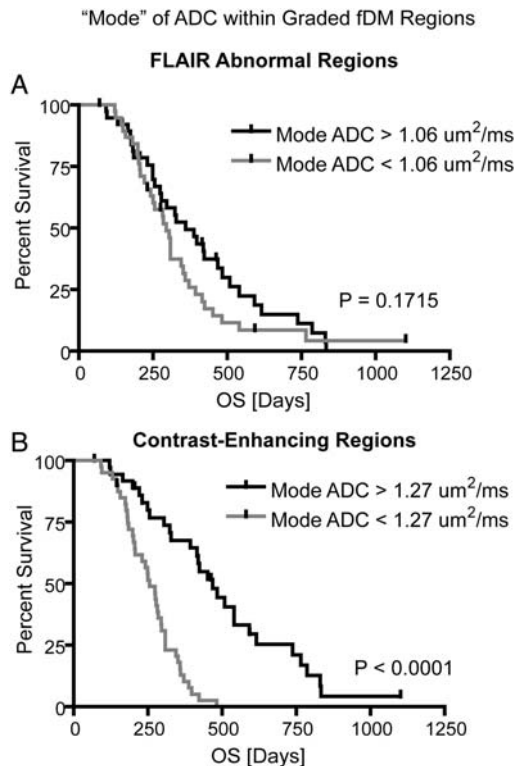


Fig. 5. Kaplan–Meier curves showing effect of combining graded fDMs with pretreatment ADC distribution information on predicting OS. (A) Mode of ADC for pretreatment ADC distributions in graded fDM–classified regions within FLAIR ROIs shows no survival difference (log-rank,  $P = .1715$ ). (B) Mode of ADC for pretreatment ADC distributions in graded fDM–classified regions within contrast enhancing ROIs demonstrates a significant survival advantage for patients with “high mode” compared with “low mode” patients (log-rank,  $P < .0001$ ; median OS: 255 vs. 468 d).

fDM-classified regions inside FLAIR are *not* predictive of OS, whereas the ADC characteristics within fDM-classified regions in contrast-enhancing regions appear to be synergistically predictive of OS when compared with fDM metrics alone. Our results suggest that graded fDM–defined regions reflect a significantly different subpopulation of voxels than does either traditional fDM–defined regions or the entire ROI. These results have 2 fundamental implications. First, they demonstrate that graded fDM–defined pretreatment ADC characteristics are significantly different than pretreatment ADC characteristics in the entire ROI, which has previously been shown to be predictive of progression-free survival in patients treated with bevacizumab.<sup>24</sup> Secondly, these results demonstrate that graded fDM–derived ADC characteristics are significantly different from traditional fDM–derived ADC characteristics, thus suggesting some added benefit of performing a graded voxel classification. Taken together, our results suggest that fDMs should be calculated preferentially in contrast-enhancing regions, when observed, since contrast-enhancing regions are likely to

contain a greater percentage of solid tumor and thus have been found to be more predictive of OS compared with fDMs applied to FLAIR ROIs. It is important to note that the particular thresholds used for patient stratification (median values) may be dependent on the particular patient population used and were chosen primarily to illustrate survival-difference “high” and “low” ADC or fDM volume groups.

#### Other Imaging Biomarkers for Anti-Angiogenic Therapy

Recently, multiple imaging biomarkers have been explored for use in predicting the response of gliomas to anti-angiogenic therapies. In a pilot study involving the use of [ $^{18}\text{F}$ ]-fluorothymidine PET to image cell proliferation during treatment with bevacizumab and irinotecan, investigators reported a significant survival advantage in patients, with more than a 25% reduction in tracer uptake compared with baseline.<sup>26</sup> In a separate study involving the use of dynamic contrast-enhanced MRI combined with specific blood serum markers to evaluate patients treated with the anti-angiogenic agent cediranib after recurrent GBM, investigators reported a significant survival advantage in patients, showing a decrease in  $K^{trans}$ , an MR-derived measure of blood vessel permeability, compared with pretreatment baseline levels.<sup>27</sup> Also, a study involving the use of a pretreatment ADC histogram as a predictive tool for response to bevacizumab demonstrated a significantly shorter progression-free survival in patients with low ADC prior to treatment.<sup>24</sup> In the current study we report that graded fDMs can also identify patients at risk for early tumor recurrence, and information regarding pretreatment ADC distributions can synergistically add to this predictability with better accuracy than other advanced imaging techniques. Although a few imaging biomarkers have shown early promise for predicting the response of gliomas to anti-angiogenic therapies, multicenter studies aimed at validating these biomarkers with the same clinical endpoints are necessary to determine which are the most advantageous.<sup>28</sup>

#### Technical Limitations and Considerations

An inherent advantage of the proposed graded fDM technique is the use of standard, clinical diffusion MRI scans for analysis, which allows for retrospective comparison with standard MRIs or other advanced image techniques during controlled, multicenter clinical trials. Despite this advantage, the use of standard, clinical diffusion MR sequence parameters also poses some potential limitations. For example, proper choice of  $b$ -values used to accurately estimate ADC is an important aspect of fDM implementation that must be further addressed. Per the recommendations of the National Cancer Institute Diffusion MRI Consensus Conference,<sup>29</sup> 3 or more  $b$ -values ( $0 \text{ s}/\text{mm}^2$ ,  $>100 \text{ s}/\text{mm}^2$ , and  $>500 \text{ s}/\text{mm}^2$ ) should be used for estimation of perfusion-insensitive ADC. Unfortunately, the current study was performed

retrospectively, and so the consensus recommendations could not be implemented. Additionally, the use of standard, clinical diffusion MR sequences in fDM analysis can be confounded by other pathologies; therefore, clinical use of fDMs should involve integration of interpretations from various specialists to rule out the possibility of confounding factors.

An additional limitation to the current technique is the use of a rigid-body image transformation in order to register serial diffusion MR images to the baseline images. Significant mass effect from tumor growth or intracranial pressure induced by edema may cause inaccuracies in the registration between diffusion MRI datasets. Suspected tumor regions near gyri, sulci, or the ventricles should be considered with caution, since erroneous results in these regions can occur as a result of misregistration. To overcome these challenges, we chose to use 2 sequential automated registration steps, followed by manual inspection. In addition, we excluded regions suspected of containing cerebrospinal fluid contamination from image misregistration near boundaries of tissue mismatch. An additional step of elastic (nonlinear) registration may be beneficial for the registration of significantly distorted datasets, such as the ART algorithm developed and tested by Ardekani et al.<sup>30</sup>

Another limitation to the current study was the inability to control the timing of pre- and posttreatment MR acquisitions. Studies have shown that in antiangiogenic therapies, the timing of MR acquisitions is particularly important for prediction of response.<sup>31</sup> Despite the retrospective nature of the current study, our results demonstrate that ADC maps collected 1.5 weeks prior to and 6 weeks following initial treatment with bevacizumab allow for strong prediction of patient survival.

The presence of pseudoprogression and/or treatment-induced necrosis in the presence of recurrent GBM is a potential confound to the current study. Bevacizumab has been shown to reduce edema and enhancement in pseudoprogression and treatment-induced necrosis, just as it does in cases of tumor recurrence.<sup>32</sup> Since both pseudoprogression and treatment-induced necrosis are associated with better survival compared with tumor recurrence, it is conceivable that the observed differences in survival in our cohorts may reflect different degrees of pseudoprogression and/

or treatment-induced necrosis independent of bevacizumab response. To reduce the risk of this potential confound, we chose to exclude patients who received bevacizumab within 3 months of completing radiotherapy, since pseudoprogression typically occurs within the first few months following radiotherapy.<sup>33</sup> Additionally, more than half of our patients had pathological confirmation of tumor progression, and more than 60% of the patients were administered bevacizumab 12 months after completion of radiotherapy. In patients who did not receive pathological confirmation of tumor recurrence, evidence of abnormal uptake on <sup>18</sup>F-FDOPA PET was used in combination with clinical decline and lesion growth on conventional MRI to determine tumor progression. This combination of pathology, imaging criterion, and clinical evaluation likely reduced the incidence of pseudoprogression and/or treatment-induced necrosis; however, this is still a potential confound.

## Conclusion

In summary, our results suggest that both traditional and graded fDMs applied to either FLAIR or contrast-enhancing regions were predictive of OS. Further, our results suggest that the use of graded fDMs has potential to serve as a sensitive imaging biomarker for OS in patients with recurrent GBM treated with bevacizumab and that patients having low pretreatment ADC values within the fDM-classified regions are at an even higher risk for shortened survival.

*Conflict of interest statement.* None declared.

## Funding

Brain Tumor Funder's Collaborative (W.B.P.); Art of the Brain (T.F.C.); Ziering Family Foundation in memory of Sigi Ziering (T.F.C.); Singleton Family Foundation (T.F.C.); Clarence Klein Fund for Neuro-Oncology (T.F.C.); NIH/NCI R21-CA109820 (K.M.S.); NIH/NCI R01-CA082500 (K.M.S.); MCW Advancing Healthier Wisconsin/Translational Brain Tumor Research Program (K.M.S.).

## References

1. Stupp R, Mason WP, van den Bent MJ, et al. Radiotherapy plus concomitant and adjuvant temozolomide for glioblastoma. *N Engl J Med.* 2005;352(10):987–996.
2. Wong ET, Hess KR, Gleason MJ, et al. Outcomes and prognostic factors in recurrent glioma patients enrolled onto phase II clinical trials. *J Clin Oncol.* 1999;17(8):2472–2478.
3. Plate KH, Breier G, Risau W. Molecular mechanisms of developmental and tumor angiogenesis. *Brain Pathol.* 1994;4(3):207–218.
4. Millauer B, Shawver LK, Plate KH, Risau W, Ullrich A. Glioblastoma growth inhibited in vivo by a dominant-negative Flk-1 mutant. *Nature.* 1994;367(6463):576–579.
5. Holash J, Maisonpierre PC, Compton D, et al. Vessel cooption, regression, and growth in tumors mediated by angiopoietins and VEGF. *Science.* 1999;284(5422):1994–1998.
6. Nghiemphu PL, Liu W, Lee Y, et al. Bevacizumab and chemotherapy for recurrent glioblastoma: a single-institution experience. *Neurology.* 2009;72(14):1217–1222.
7. Vredenburgh JJ, Desjardins A, Herndon JE, et al. Phase II trial of bevacizumab and irinotecan in recurrent malignant glioma. *Clin Cancer Res.* 2007;13:1253–1259.

8. Friedman AH, Prados MD, Wen PY, et al. Bevacizumab alone and in combination with irinotecan in recurrent glioblastoma. *J Clin Oncol.* 2009;27(28):4733–4740.
9. Macdonald DR, Cascino TL, Schold SC, Jr, Cairncross JG. Response criteria for phase II studies of supratentorial malignant glioma. *J Clin Oncol.* 1990;8(7):1277–1280.
10. Iwamoto FM, Abrey LE, Beal K, et al. Patterns of relapse and prognosis after bevacizumab failure in recurrent glioblastoma. *Neurology.* 2009;73(15):1200–1206.
11. Norden AD, Young GS, Setayesh K, et al. Bevacizumab for recurrent malignant gliomas: efficacy, toxicity, and patterns of recurrence. *Neurology.* 2008;70(10):779–787.
12. Moffat BA, Chenevert TL, Lawrence TS, et al. Functional diffusion map: A noninvasive MRI biomarker for early stratification of clinical brain tumor response. *Proc Nat Acad Sci.* 2005;102(15):5524–5529.
13. Moffat BA, Chenevert TL, Meyer CR, et al. The functional diffusion map: An imaging biomarker for the early prediction of cancer treatment outcome. *Neoplasia.* 2006;8(4):259–267.
14. Hamstra DA, Chenevert TL, Moffat BA, et al. Evaluation of the functional diffusion map as an early biomarker of time-to-progression and overall survival in high-grade glioma. *Proc Nat Acad Sci.* 2005;102(46):16759–16764.
15. Hamstra DA, Galbán CJ, Meyer CR, et al. Functional diffusion map as an early imaging biomarker for high-grade glioma: correlation with conventional radiologic response and overall survival. *J Clin Oncol.* 2008;26(10):3387–3394.
16. Ellingson BM, Rand SD, Malkin MG, Schmainda KM. Utility of functional diffusion maps to monitor a patient diagnosed with gliomatosis cerebri. *J Neurooncol.* 2010;97(3):419–423.
17. Ellingson BM, Malkin MG, Rand SD, et al. Validation of functional diffusion maps (fDMs) as a biomarker for human glioma cellularity. *J Magn Reson Imaging.* 2010;31(3):538–548.
18. Ellingson BM, Malkin MG, Rand SD, Bedekar DP, Schmainda KM. Functional diffusion maps applied to FLAIR abnormal areas are valuable for the clinical monitoring of recurrent brain tumors. *Proc Intl Soc Mag Reson Med.* 2009;17:285.
19. Ellingson BM, Malkin MG, Rand SD, et al. Comparison of cytotoxic and anti-angiogenic treatment responses using functional diffusion maps in FLAIR abnormal regions. *Proc Intl Soc Mag Reson Med.* 2009;17:1010.
20. Ellingson BM, Malkin MG, Rand SD, et al. Volumetric analysis of functional diffusion maps (fDMs) is a predictive imaging biomarker for cytotoxic and anti-angiogenic treatments in malignant gliomas. *J Neurooncol.* 2011;102:95–103.
21. Reese TG, Heid O, Weisskoff RM, Wedeen VJ. Reduction of eddy-current-induced distortion in diffusion MRI using a twice-refocused spin echo. *Magn Reson Med.* 2003;49(1):177–182.
22. Cox RW, Jesmanowicz A. Real-time 3D image registration for functional MRI. *Magn Reson Med.* 1999;42:1014–1018.
23. de Groot JF, Fuller G, Kumar AJ, et al. Tumor invasion after treatment of glioblastoma with bevacizumab: radiographic and pathologic correlation in humans and mice. *Neuro Oncol.* 2010;12(3):233–242.
24. Pope WB, Kim HJ, Huo J, et al. Recurrent glioblastoma multiforme: ADC histogram analysis predicts response to bevacizumab treatment. *Radiology.* 2009;252(1):182–189.
25. Zuniga RM, Torcuator R, Jain R, et al. Efficacy, safety and patterns of response and recurrence in patients with recurrent high-grade gliomas treated with bevacizumab plus irinotecan. *J Neurooncol.* 2009;91(3):329–335.
26. Chen W, Delaloye S, Silverman DH, et al. Predicting treatment response of malignant gliomas to bevacizumab and irinotecan by imaging proliferation with [18F] fluorothymidine positron emission tomography: a pilot study. *J Clin Oncol.* 2007;25(30):4714–4721.
27. Sorensen AG, Batchelor TT, Zhang WT, et al. A "vascular normalization index" as potential mechanistic biomarker to predict survival after a single dose of cediranib in recurrent glioblastoma patients. *Cancer Res.* 2009;69(13):5296–5300.
28. Jain RK, Duda DG, Willett CG, et al. Biomarkers of response and resistance to antiangiogenic therapy. *Nat Rev Clin Oncol.* 2009;6(6):327–338.
29. Padhani AR, Liu G, Mu-Koh D, et al. Diffusion-weighted magnetic resonance imaging as a cancer biomarker: consensus and recommendations. *Neoplasia.* 2009;11(2):102–125.
30. Ardekani BA, Guckemus S, Bachman A, Hoptman MJ, Wojtasek M, Nierenberg J. Quantitative comparison of algorithms for inter-subject registration of 3D volumetric brain MRI scans. *J Neurosci Methods.* 2005;142(1):67–76.
31. Gerstner ER, Chen PJ, Wen PY, Jain RK, Batchelor TT, Sorensen AG. Infiltrative patterns of glioblastoma spread detected via diffusion MRI after treatment with cediranib. *Neuro Oncol.* 2010;12(5):466–472.
32. Gonzalez J, Kumar AJ, Conrad CA, Levin VA. Effect of bevacizumab on radiation necrosis of the brain. *Int J Radiat Oncol Biol Phys.* 2007;67(2):323–326.
33. Brandsma D, Stalpers L, Taal W, Sminia P, van den Bent MJ. Clinical features, mechanisms, and management of pseudoprogression in malignant gliomas. *Lancet Oncol.* 2008;9(5):453–461.